J. Phys. Chem. A **2001,** *105,* 9717−9724

Quantum Mechanical Study of the Competitive Hydration between Protonated Quinazoline and Li^+, Na^+, and Ca^{2+} Ions

Phillip Sawunyama*,† and George W. Bailey‡

National Research Council, U.S. Environmental Protection Agency, Athens, Georgia 30605, and Ecosystems Research Division, National Exposure Research Laboratory, U.S. Environmental Protection Agency, Athens, Georgia 30605

Received: March 13, 2001; In Final Form: June 1, 2001

Hydration reactions are fundamental to many biological functions and environmental processes. The energetics of hydration of inorganic and organic chemical species influences their fate and transport behavior in the environment. In this study, gas-phase quantum mechanical calculations at the MP2/6-31G**//HF/6-31G* and B3LYP/6-311+G(2df,2p)//B3LYP/6-31G* levels of theory are used to interpret the local competition for water between protonated quinazoline (1,3-diazanaphthalene) and metal ions, i.e., Li^+, Na^+, and Ca^{2+}, under very low water contents. Calculated enthalpies and free energies of hydration at 298.15 K, $\Delta H_{hyd}{}^{298}$ and $\Delta G_{hyd}{}^{298}$, respectively, for the reactions quinazoline + H_2O → quinazoline hydrate and $M^{z+} + H_2O \rightarrow M(H_2O)^{z+}$ show that hydration of metal ions is more favorable than hydration of the quinazoline species. At the MP2/6-31G**//HF/6-31G* computational level, $\Delta H_{hyd}{}^{298}$ values range from 0.4 kcal mol^{-1} for neutral quinazoline to −11.1 and −10.5 kcal mol^{-1} for N1 and N3 protonated quinazoline monocations, respectively, while $\Delta H_{hyd}{}^{298} = -39.3$, −28.2, and −56.4 kcal mol^{-1} for Li^+, Na^+, and Ca^{2+} ions, respectively. At the B3LYP/6-311+G(2df,2p)//B3LYP/6-31G* computational level, $\Delta H_{hyd}{}^{298} = 6.9$, −5.5, and −5.4 kcal mol^{-1} for neutral quinazoline, N1, and N3 protonated quinazoline monocations, respectively, while $\Delta H_{hyd}{}^{298}$ values are −34.0, −23.4, and −55.7 kcal mol^{-1}for Li^+, Na^+, and Ca^{2+} ions, respectively. Accordingly, $\Delta G_{hyd}{}^{298}$ values indicate that although metal cations hydrate spontaneously, quinazoline species do not. In addition to hydration, direct reaction between quinazoline species and metal cations is also explored.

Introduction

Hydration is a subject of both fundamental and practical importance. For example, hydration influences many aspects of biological functions such as enzyme catalysis and the folding, conformational stability, and binding specificity of proteins.[1−6] Electrochemical and other industrially important processes such as the gelatinization of starch[7] and the dynamical properties of cellulose acetate[8] are governed by hydration phenomena. In geochemistry and soil science, the relative extents and free energies of hydration of ions at the clay−water interface play crucial roles in determining the course of surface reactions involving clay counterions.[9−13] Under low water contents, the interactions at clay−water interfaces involve local competitive-type hydration processes between simple clay counterions such as Na^+, K^+, Mg^{2+}, and Ca^{2+} ions. However, the scenario is somewhat disturbed if an organic compound or other metal ion is introduced. Introduction of a foreign species to the clay−water system perturbs the equilibria and dynamics of hydration of counterions with a concomitant competition for water between the counterions and the foreign species. This has important implications in the fate and transport behavior of organic pollutants as well as heavy metal ions in the environment.

To understand the fundamental processes involved in competitive hydration reactions at clay−water interfaces, molecular probes that undergo reversible hydration at the surface are required. One such probe is quinazoline (1,3-diazanaphthalene). In acidic aqueous solutions, quinazoline will rapidly undergo protonation to form several cation species. These in turn undergo reversible covalent hydration across the N(3)═C(4) double bond, and at equilibrium the main species is the hydrated cation species, 3,4-dihydro-4-hydroxyquinazolin-1-ium ion (Figure 1).[14−19] In the early 1970s, the quinazoline reaction was used to probe hydration at the Na−montmorillonite surface.[20] Near the clay surface, an inhibition of the hydration of quinazoline was observed. This phenomenon was attributed to a local competition between quinazoline and inorganic cations for water of hydration.

Although there have been many experimental investigations on the hydration of quinazoline,[14−19] there have been very few theoretical studies.[21,22] The theoretical calculations treated the hydration reactions at the semiempirical level, i.e., using Hückel molecular orbital calculations,[21] complete neglect of differential overlap (CNDO) and the intermediate neglect of differential overlap (INDO) wave functions.[22] Chemical reactivity of the various species was explained in terms of electron densities, bond orders, and van der Waals interaction energies. Quantum mechanical and free energy perturbation methods were also applied to the study of the covalent hydration of carbonyl-containing compounds[23] and heteroaromatic compounds (−C═N− double bond).[24] Nonetheless, in comparison with studies on the hydration of organic compounds, the interaction of water with metal cations has been treated extensively at both the experimental and quantum mechanical computational levels.[1,9−13,24−34]

---

* To whom correspondence should be addressed. Fax: (706)-355-8202. E-mail: sawunyama.phillip@epa.gov.

† National Research Council.

‡ Ecosystems Research Division, National Exposure Research Laboratory.

10.1021/jp0109527 CCC: \$20.00

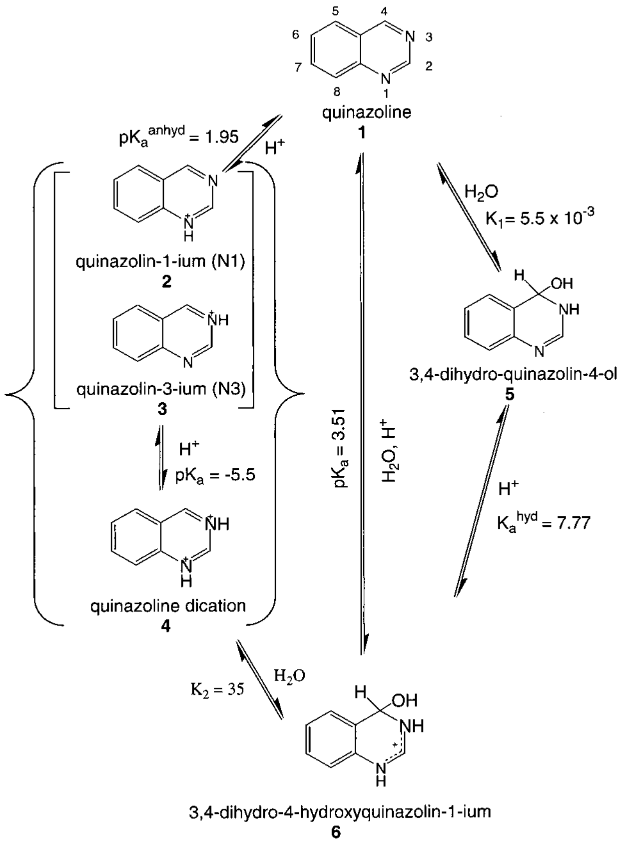

Figure 1. Summary of processes involved in the uncatalyzed hydration of quinazoline species. Equilibrium constant data are from refs 14−19.

To our knowledge, competitive hydration reactions involving metal cations and quinazoline species have not been investigated theoretically at a variety of computational levels. In the work described herein, we explored the competitive hydration reactions involving quinazoline species and metal cations at the Hartree−Fock (HF) level with electron correlation treated at the second-order Møller−Plesset perturbation (MP2) level,[35−38] and at the density functional theory (DFT) level[39] with Becke's three-parameter hybrid functional[40] using the Lee−Yang−Parr[41] correlational functional (B3LYP). The pathways of the reactions were investigated in depth by calculating proton affinities, enthalpies of hydration at 298.15 K ($\Delta H_{\mathrm{hyd}}^{298}$), free energies at 298.15 K ($\Delta G_{\mathrm{hyd}}^{298}$), and activation energies for several quinazoline species that are considered to be present in acidic aqueous solutions as well as $\Delta H_{\mathrm{hyd}}^{298}$ and $\Delta G_{\mathrm{hyd}}^{298}$ for the hydration of the metal cations.

Computational Methods

All calculations were performed using the Gaussian 98 suite of programs[42] running on a Silicon Graphics Octane desktop workstation and on a PC. Further, all calculations are for 0 K structures. The reactions were initially studied at the restricted closed-shell Hartree−Fock (RHF) level using the 6-31G* and the 6-31G** polarization basis sets[43−45] stored internally in the Gaussian 98 program. The HF geometry optimizations employed the 6-31G* basis set. Quinazoline, quinazolin-1-ium (N1 monocation), quinazolin-3-ium (N3 monocation), dication, and metal−quinazoline species were optimized within the C_s point group (planar). Quinazoline hydrates (3,4-dihydroquinazolin-4-ol and 3,4-dihydro-4-hydroxyquinazolin-1-ium) and metal−quinazoline hydrate complexes were nonplanar with C_1 symmetry. Metal cation−water complexes had C_{2v} symmetry. Stationary points were characterized by performing frequency calculations at the same level of theory and the zero-point energies (ZPEs) were scaled by 0.8929. Final energy calculations were performed at the Møller−Plesset second-order perturbation theory frozen core approximation (MP2−FC) with the 6-31G** basis set. Activation energies for the reversible hydration of neutral and protonated quinazoline species were calculated as follows. The transition structures were located using the synchronous transit-guided quasi-Newton method[46,47] at the HF/6-31G* level. The method uses a quadratic synchronous transit approach to get closer to the quadratic region of the transition state and then uses a quasi-Newton or eigenvector-following algorithm to complete the optimization. The stationary points were then characterized as described above. The intrinsic reaction path or intrinsic reaction coordinate (IRC) connecting the reactants through the transition state was examined by performing reaction path following calculations[48,49] at the HF/6-31G* level of theory. Final energy calculations for the transition structures were performed at the MP2/6-31G** level of theory.

Density functional calculations were performed using Becke's three-parameter hybrid functional using the Lee, Yang, and Parr correlational functional (B3LYP).[40,41] The B3LYP method was demonstrated to give high-accuracy results for the hydration of metal cations.[31,37] Moreover, density functional methods include the effects of electron correlation and very large basis sets can be used for the same amount of computation resources as Hartree−Fock theory. The structures (vide supra) were optimized at the restricted closed-shell B3LYP using the 6-31G* basis set. Frequency calculations preformed at the same level of theory were used to characterize stationary points and the zero-point energies (ZPEs) were scaled by 0.9804. Final energy calculations were performed using a very large basis set, i.e., 6-311+G(2df,2p).[50−53] Likewise, transition structures were located using the synchronous transit-guided quasi-Newton method[46,47] at the B3LYP/6-31G* level and the reaction path connecting the reactants through the transition state was examined by performing reaction path following (IRC) calculations[48,49] at the B3LYP/6-31G* level of theory. The nature of the stationary point was characterized by performing frequency calculations at the same level of theory.

Results

Optimized geometrical parameters of quinazoline species at HF/6-31G* and B3LYP/6-31G* levels of theory were generally different. For example, bond lengths obtained at the HF/6-31G* level were normally shorter than those obtained at the B3LYP/6-31G* level. Selected bond lengths (pyrimidine ring) are presented in Table 1. Covalent hydration across the N(3)−C(4) bond destroyed aromaticity within the pyrimidine ring and the resulting resonance effects are described below.

In Table 2, the total molecular energies of the various species at the HF/6-31G**//HF/6-31G*, MP2/6-31G**//HF/6-31G*, and B3LYP/6-311+(2df,2p)//B3LYP/6-31G* computational levels and the corresponding zero-point energies at the HF/6-31G*//HF/6-31G* and B3LYP/6-31G*//B3LYP/6-31G* computational levels, respectively, are presented. Molecular energies at the HF/6-31G**//HF/6-31G* computational level are included for comparison purposes.

Proton Affinities. Many experimental studies revealed that hydration of quinazoline is pH dependent.[14−19] At pHs below 7, protonation of quinazoline (quinazoline + $H^+ \rightarrow$ quinazoline cation) precedes hydration, whereas at neutral or pHs greater than 7, protonation is not a precondition for hydration. Normally,

TABLE 1: Some Optimized Bond Lengths for the Quinazoline Species

		r(N(1)−C(2)) (Å)		r(C(2)−N(3)) (Å)		r(N(3)−C(4)) (Å)	
	symmetry	HF/6-31G*	B3LYP/6-31G*	HF/6-31G*	B3LYP/6-31G*	HF/6-31G*	B3LYP/6-31G*
quinazoline	C_s	1.319	1.315	1.311	1.363	1.313	1.317
N1 monocation	C_s	1.319	1.340	1.311	1.326	1.313	1.331
N3 monocation	C_s	1.270	1.294	1.369	1.382	1.323	1.339
dication	C_s	1.296	1.319	1.332	1.349	1.351	1.359
3,4-dihydroquinazolin-4-ol	C_1	1.261	1.287	1.363	1.372	1.439	1.452
3,4-dihydro-4-hydroxyquinazolin-1-ium	C_1	1.299	1.318	1.301	1.320	1.477	1.492

TABLE 2: Total Molecular Energies and Zero-Point Energies[a]

molecule	HF/6-31G**// HF/6-31G*	MP2/6-31G**// HF/6-31G*	ZPE[b]	B3LYP/6-311+G(2df,2p)// B3LYP/6-31G*	ZPE[c]
A.Quinazoline Species at the Various Computational Levels					
quinazoline	−415.350544	−416.705761	0.133702	−418.101448	0.121905
N1 monocation	−415.734520	−417.078657	0.147942	−418.467567	0.135204
N3 monocation	−415.732439	−417.079580	0.147960	−418.467738	0.135181
dication	−415.936363	−417.274480	0.161646	−418.663757	0.148023
3,4-dihydroquinazolin-4-ol	−491.376439	−492.929521	0.163638	−494.557178	0.148746
3,4-dihydro-4-hydroxyquinazolin-1-ium	−491.775184	−493.321322	0.178494	−494.943635	0.162682
B. Metal Cations, Metal−Hydrate Complexes, Metal−Quinazolinehydrate Cation Complexes, Metal−Quinazoline Complexes, and Water at the Various Computational Levels					
Li^+	−7.235537	−7.235537		−7.284918	
$Li(H_2O)^+$	−83.322202	−83.519954	0.026255	−83.804014	0.023950
$Li[C_8H_9N_2O]^{2+}$	−498.966778	−500.515228	0.180565	−502.178958	0.164728
$Li[C_8H_6N_2]^+$	−422.665486	−424.020159	0.135783	−425.459055	0.124009
Na^+	−161.659288	−161.659288		−162.087568	
$Na(H_2O)^+$	−237.728335	−237.925640	0.025564	−238.589290	0.023227
$Na[C_8H_9N_2O]^{2+}$	−653.376694	−654.924107	0.179788	−656.968323	0.16381
$Na[C_8H_6N_2]^+$	−577.066970	−578.422106	0.134802	−580.239413	0.123082
Ca^{2+}	−676.104056	−676.112275		−676.905785	
$Ca(H_2O)^{2+}$	−752.216556	−752.423752	0.026010	−753.459230	0.023769
$Ca[C_8H_9N_2O]^{3+}$	−1167.792856	−1169.351496	0.179634	−1171.772928	0.163643
$Ca[C_8H_6N_2]^{2+}$	−1091.582709	−1092.9498665	0.134577	−1095.152231	0.122683
water	−76.023571	−76.219366	0.022972	−76.462413	0.020749

[a] All energies in hartrees. [b] Zero-point energy calculated at HF/6-31G*//HF/6-31G*. [c] Zero-point energy calculated at B3LYP/6-31G*//B3LYP/6-31G*.

TABLE 3: Proton Affinities for Quinazoline Species at 0 K

	PA (ΔE_{zpc}, kcal mol^{-1})[a]		
reaction	HF/6-31G**// HF/6-31G*	MP2/6-31G**// HF/6-31G*	B3LYP/6-311+G(2df,2p)// B3LYP/6-31G*
$C_8H_6N_2 + H^+ \rightarrow C_8H_7N_2^+$ (**1** → **2**)	232.0	225.1	221.4
$C_8H_6N_2 + H^+ \rightarrow C_8H_7N_2^+$ (**1** → **3**)	230.7	225.6	221.5
$C_8H_6N_2 + 2H^+ \rightarrow C_8H_8N_2^{2+}$ (**1** → **4**)	350.1	339.3	336.5
$C_8H_7N_2^+ + H^+ \rightarrow C_8H_8N_2^{2+}$ (**2** → **4**)	118.1	114.3	115.1
$C_8H_7N_2^+ + H^+ \rightarrow C_8H_8N_2^{2+}$ (**3** → **4**)	119.4	113.7	115.0
$C_8H_8N_2O + H^+ \rightarrow C_8H_9N_2O^+$ (**5** → **6**)	240.9	236.5	233.8

[a] E_{zpc} is zero-point energy corrected proton affinity.

in acidic solutions, the attacking species is water, but in neutral or basic conditions the attacking species is the hydroxyl anion. Thus, in acidic solutions the stability of the quinazoline cation species determines the course of the hydration reaction. The calculated proton affinities (PAs) at 0 K for quinazoline are presented in Table 3. Compared with PAs computed at the B3LYP/6-311+G(2df,2p)//B3LYP/6-31G* level of theory, PAs computed at the MP2/6-31G**//HF/6-31G* level of theory were generally higher by about 3 kcal mol^{-1}. The HF/6-31G**//HF-6-31G* computational level overestimated PAs by on average 6 kcal mol^{-1}. Nonetheless, both the B3LYP/6-311+G(2df,2p)//B3LYP/6-31G* and the MP2/6-31G**//HF/6-31G* computational levels indicate that protonation of quinazoline produces three stable species whose relative stability is in the order dication ≫ N3 monocation > N1 monocation. Remarkably, the energy difference between the N3 and N1 monocations is only 0.5 kcal mol^{-1} at the MP2/6-31G**//HF/6-31G* level and is even smaller, i.e., 0.1 kcal mol^{-1}, at the B3LYP/6-311+G(2df,2p)//B3LYP/6-31G* level. As such, both N1 and N3 monocations can coexist in solution. In contrast, the HF/6-31G**//HF/6-31G* level predicts that the N1 monocation is more stable than the N3 monocation. This discrepancy is probably due to the use of a small basis set and lack of treatment of electron correlation effects at the HF level. Protonation to the dication results in further stabilization of the quinazoline species; however, this process is expected to compete with hydration to form the 3,4-dihydro-4-hydroxyquinazolin-1-ium ion. Interestingly, protonation of the neutral quinazoline hydrate results in an energy of stabilization of 236.5 kcal mol^{-1} and 233.8 kcal mol^{-1} at the MP2/6-31G**//HF/6-31G* and B3LYP/6-311+G(2df,2p)//B3LYP/6-31G* computational levels, respectively.

Quinazoline Metal Affinity (MA). In a quinazoline−metal ion system, the metal affinity (MA) reaction, i.e., quinazoline + $M^{z+} \rightarrow M[\text{quinazoline}]^{z+}$, may compete with protonation. Calculated quinazoline MAs (attack on position N(3)) for Li^+, Na^+, and Ca^{2+} cations, respectively, are listed in Table 4. All

TABLE 4: Quinazoline−Metal Cation Affinity at 0 K[a]

	MA(kcal mol^{-1})		
reaction	HF/6-31G**// HF/6-31G*	MP2/6-31G**// HF/6-31G*	B3LYP/6-311+G(2df,2p)// B3LYP/6-31G*
$C_8H_6N_2 + Li^+ \rightarrow Li[C_8H_6N_2]^+$	48.5	48.2	44.3
$C_8H_6N_2 + Na^+ \rightarrow Na[C_8H_6N_2]^+$	35.2	35.1	30.9
$C_8H_6N_2 + Ca^{2+} \rightarrow Ca[C_8H_6N_2]^{2+}$	79.8	82.2	90.5

[a] Metal affinities have been zero-point energy corrected.

TABLE 5: ΔH_{hyd}^{298} and ΔG_{hyd}^{298} for the Hydration of Quinazoline Species and Metal Cations

	ΔH_{hyd}^{298} (kcal mol^{-1})				ΔG_{hyd}^{298} (kcal mol^{-1})		
reaction	HF	MP2	B3LYP	literature[a]	HF	MP2	B3LYP
$C_8H_6N_2 + H_2O \rightarrow C_8H_8N_2O$	1.7	0.4	6.9		12.9	11.6	17.6
$C_8H_7N_2^+ + H_2O \rightarrow C_8H_9N_2O$ (N1)	−7.2	−11.1	−5.5		3.9	0.0	5.2
$C_8H_7N_2^+ + H_2O \rightarrow C_8H_9N_2O$ (N3)	−8.5	−10.5	−5.4		2. 6	0.6	5.3
$Li^+ + H_2O \rightarrow Li(H_2O)^+$	−38.0	−39.3	−34.0	−34.0	−40.6	−41.9	−37.1
$Na^+ + H_2O \rightarrow Na(H_2O)^+$	−27.2	−28.2	−23.4	−24.0	−31.2	−32.1	−27.8
$Ca^{2+} + H_2O \rightarrow Ca(H_2O)^{2+}$	−54.4	−56.4	−55.7		−58.5	−60.2	−60.2

[a] Reference 1.

levels of theory predict the same trend in cation affinity, i.e., $Ca^{2+} > Li^+ > Na^+$. Compared to proton addition, stabilization of quinazoline on account of metal cation addition is small, however. For example, at the MP2 level, PA = 225.6 kcal mol^{-1} whereas MA = 48.2, 35.1, and 82.2 kcal mol^{-1} for Li^+, Na^+, and Ca^{2+}, respectively. Accordingly, at the B3LYP level, PA = 221.5 kcal mol^{-1} whereas MA = 44.3, 30.9, and 90.5 kcal mol^{-1} for Li^+, Na^+, and Ca^{2+}, respectively. These data show that in acidic aqueous solutions, protonation of quinazoline followed by covalent hydration is energetically more favorable than metal cation addition.

Hydration Reactions. The enthalpies and free energies of hydration at 298.15 K, ΔH_{hyd}^{298} and ΔG_{hyd}^{298}, respectively, for the reactions Quinazoline + H_2O → Quinazoline hydrate and $M^{z+} + H_2O \rightarrow M(H_2O)^{z+}$ at the different computational levels are given in Table 5. At the MP/6-31G**//HF/6-31G* level, ΔH_{hyd}^{298} values range from 0.4 kcal mol^{-1} for hydration of neutral quinazoline to −11.1 and −10.5 kcal mol^{-1} for hydration of N1 and N3 cations, respectively. Compared to ΔH_{hyd}^{298} for quinazoline cation species, ΔH_{hyd}^{298} values for the metal cations are larger by factors of ∼3−6. At the B3LYP/6-311+G(2df,2p)//B3LYP/6-31G* level, ΔH_{hyd}^{298} for neutral quinazoline is much larger than that obtained at the MP2 level. Even so, ΔH_{hyd}^{298} for N1 and N3 monocations are approximately half the values calculated at the MP2 level. Remarkably, ΔH_{hyd}^{298} values for the metal cations are on the order of 4−10-fold larger than those for the quinazoline cation species. It should be noted that calculated ΔH_{hyd}^{298} values for Li^+ and Na^+ ions at the B3LYP/6-311+G(2df,2p)//B3LYP/6-31G* level are in agreement with experimental values within the estimated experimental uncertainty. Finally, ΔG_{hyd}^{298} for quinazoline species were generally positive whereas ΔG_{hyd}^{298} for the metal cations were negative.

Enthalpy of Formation of Metal−Quinazoline Hydrate Complexes. In addition to quinazoline metal cation affinity (MA), in the event of an excess of 3,4-dihydro-4-hydroxyquinazolin-1-ium ions, complexation of 3,4-dihydro-4-hydroxyquinazolin-1-ium ions with metal cations, a reaction that can be represented as $M^{z+} + C_8H_9N_2O^+ \rightarrow M[C_8H_9N_2O]^{z+1}$, is also possible. This process may be envisaged as the metal cation affinity of the 3,4-dihydro-4-hydroxyquinazolin-1-ium ion. Calculated enthalpies of formation, ΔH_f^{298}, of the various metal−3,4-dihydro-4-hydroxyquinazolin-1-ium ion complexes, are collected in Table 6. Clearly, given that there are many other favorable competing reactions, formation of such complexes is doubtful.

TABLE 6: ΔH_f^{298} for the Formation of Metal−Quinazoline−Hydrate Complexes

	ΔH_f^{298} (kcal mol^{-1})		
reaction	HF	MP2	B3LYP
$Li^+ + C_8H_9N_2O^+ \rightarrow Li[C_8H_9N_2O]^{2+}$	28.8	27.3	32.4
$Na^+ + C_8H_9N_2O^+ \rightarrow Na[C_8H_9N_2O]^{2+}$	37.3	36.5	40.5
$Ca^{2+} + C_8H_9N_2O^+ \rightarrow Ca[C_8H_9N_2O]^{3+}$	55.0	52.3	48.7

Bond Separation Reactions (Resonance Stabilization Energy). Bond separation energies at 0 K (ΔE) for quinazoline, N1 monocation, N3 monocation, 3,4-dihydroquinazolin-4-ol, and 3,4-dihydro-4-hydroxyquinazolin-1-ium ion were calculated at various computational levels using the isodesmic reactions in Scheme 1. For comparison purposes, the bond separation energies of benzene at the various computational levels were also calculated. The results obtained are summarized in Table 7. At the computational levels considered in this study, all the molecules are resonance stabilized by well over 100 kcal mol^{-1}. MP2/6-31G**//HF/6-31G* computational level results were generally higher than the corresponding HF/6-31G**//HF/6-31G* and B3LYP/6-311+G(2df,2p)//B3LYP/6-31G* computational level results. For example, the bond separation energy for quinazoline was calculated to be 123.2, 149.2, and 135.1 kcal mol^{-1}, at the HF, MP2, and B3LYP levels, respectively. Likewise, the bond separation energy of the 3,4-dihydro-4-hydroxyquinazolin-1-ium ion was calculated to be 142.8, 166.0, and 151.1 kcal mol^{-1} at the HF, MP2, and B3LYP levels, respectively. It should be noted that the differences in aromatic stabilization for the N1 and N3 monocations are identical to those obtained for proton stabilization, i.e., 0.6 kcal mol^{-1} at the MP2/6-31G**//HF/6-31G* level and 0.1 kcal mol^{-1} at the B3LYP/6-311G+G(2df,2p)//B3LYP/6-31G* level.

The resonance stabilization energies for the hydration of the neutral quinazoline, N1, and N3 monocations to the corresponding hydrates are shown in Table 7 ($\Delta\Delta E = \Delta E_{hydrate} - \Delta E_{anhydrous}$). Hydration of neutral quinazoline to the corresponding neutral hydrate results in loss of resonance stabilization energy of about 4.6 kcal mol^{-1} as calculated at the B3LYP/6-311G+G(2df,2p)//B3LYP/6-31G* level. Calculated results are, however, smaller at the other computational levels. Experimental studies have shown that neutral quinazoline hydrate is unstable and it reversibly dehydrates with first-order kinetics to neutral

Scheme 1

Compound	Bond Separation Reaction
quinazoline (**1**)	$C_8H_6N_2 + 10CH_4 + 2NH_3 \rightarrow 4CH_3CH_3 + 3CH_2CH_2 + 2CH_3NH_2 + 2CH_2NH$
quinazoline hydrate (**5**)	$C_8H_8N_2O + 11CH_4 + 2NH_3 \rightarrow 4CH_3CH_3 + 3CH_2CH_2 + 3CH_3NH_2 + CH_2NH + CH_3OH$
N1/N3 monocation (**2** or **3**)	$C_8H_7N_2^+ + 10CH_4 + 2NH_3 \rightarrow 4CH_3CH_3 + 3CH_2CH_2 + 2CH_2NH + CH_3NH_2 + CH_3NH_3^+$
quinazoline hydrate cation (**6**)	$C_8H_9N_2O^+ + 11CH_4 + 2NH_3 \rightarrow 4CH_3CH_3 + 3CH_2CH_2 + CH_2NH + 2CH_3NH_2 + CH_3NH_3^+ + CH_3OH$
benzene	$C_6H_6 + 6CH_4 \rightarrow 3CH_3CH_3 + 3CH_2CH_2$

TABLE 7: Calculated Bond Separation Energies (kcal mol^{-1}) at 0 K[a]

	HF/6-31G**//HF/6-31G*			MP2/6-31G**//HF/6-31G*			B3LYP/6-311+G(2df,2p)//B3LYP/6-31G*		
	ΔE (HF)	ΔE (ZPE)	ΔE (HF + ZPE)	ΔE (MP2)	ΔE (ZPE)	ΔE (MP2 + ZPE)	ΔE (B3LYP)	ΔE (ZPE)	ΔE (B3LYP + ZPE)
quinazoline hydrate	106.0	16.0	122.0	133.1	16.0	149.1	117.5	13.0	130.5
quinazoline	109.2	14.0	123.2	135.2	14.0	149.2	124.1	11.0	135.1
$\Delta\Delta E$	−3.2	2.0	−1.2	−2.1	2.0	−0.1	−6.6	2.0	−4.6
quinazoline hydrate cation	125.9	16.9	142.8	149.1	16.9	166.0	137.4	13.7	151.1
N1 cation	119.9	15.2	135.1	139.4	15.2	154.6	131.2	12.1	143.3
$\Delta\Delta E$	6.0	1.7	7.7	9.7	1.7	11.4	6.2	1.6	7.8
quinazoline hydrate cation	125.9	16.9	142.8	149.1	16.9	166.0	137.4	13.7	151.1
N3 cation	118.6	15.2	133.8	140.0	15.2	155.2	131.3	12.1	143.4
$\Delta\Delta E$	7.3	1.7	9.0	9.1	1.7	10.8	6.1	1.6	7.7
benzene	58.3	5.8	64.1	70.2	5.8	76.0	62.9	4.5	67.3

[a] Resonance energy difference $\Delta\Delta E = \Delta E(\text{hydrate}) - \Delta E(\text{anhydrous})$.[24]

quinazoline.[15] On the basis of the above result, the experimentally observed instability of neutral quinazoline hydrate is due in part to the loss in resonance stabilization energy. On the contrary, hydration of N1 and N3 monocations to the 3,4-dihydro-4-hydroxyquinazolin-1-ium ion is extensive and results in a gain of resonance stabilization energy of approximately 8 kcal mol^{-1} as calculated at the B3LYP/6-311G+(2df,2p)//B3LYP/6-31G* computational level. The corresponding resonance energy at the MP2/6-31G**//HF/6-31G* computational level is about 11 kcal mol^{-1}.

Activation Energy, E_a. We also calculated the activation energies (E_a) for the reversible hydration of neutral quinazoline and protonated quinazoline. Frequency calculations established that only one imaginary frequency existed for the transition state structures considered. Potential energy surface reaction path following calculations also confirmed the nature of the reactants and products linking the transition structure (TS). For the reversible hydration of neutral quinazoline, the computed TS imaginary frequency was −514.3 cm^{-1} at the HF/6-31G* level of theory. Accordingly, the calculated TS imaginary frequency was −485.7 cm^{-1} at the B3LYP/6-31G* level of theory. On the basis of the calculated frequencies and the single point energies, activation energies (0 K) at the MP2/6-31G**//HF/6-31G* computational level for the reversible hydration of neutral quinazoline were calculated to be 4.9 and 3.6 kcal mol^{-1} for the forward and reverse reactions, respectively. Similarly, the calculated energies at the B3LYP/6-311G+(2df,2p)//B3LYP/6-31G* level were 11.8 and 3.8 kcal mol^{-1} for the forward and reverse reactions, respectively. The reaction profile is shown in Figure 2.

In the case of hydration of protonated quinazoline species, activation energies for the forward and reverse reactions were calculated on the basis of the hydration of the N1 monocation (Figure 3). The computed TS imaginary frequency was −2074.9 cm^{-1} at the HF/6-31G* level of theory. At the B3LYP/6-31G* level of theory, the TS imaginary frequency was −1591.9 cm^{-1}. The calculated activation energies for reversible hydration of the protonated species were 28.5 and 38.8 kcal mol^{-1}, respectively, at the MP2/6-31G**//HF/6-31G* computational level. Calculated activation energies at the B3LYP/6-311G+(2df,2p)//B3LYP/6-31G* level were 35.1 and 39.4 kcal mol^{-1} for the forward and reverse reactions, respectively.

Discussion

A variety of computational methods are now routinely applied to the study of a wide range of chemical phenomena, including hydration. Depending on the theoretical model used, computational accuracy levels attained, for ionic hydration in particular,[27−29,31−34] are comparable to experimental levels. Similar trends were noted in this study. Data obtained at the HF/6-31G**//HF/6-31G* and MP2/6-31G**//HF/6-31G* levels of theory were generally overestimated by as much as 15% compared to experimental results. Calculations at the B3LYP/6-311+G(2df,2p)//B3LYP/6-31G* level improved the accuracy of the obtained results. For example, experimental[1] $\Delta H_{\text{hyd}}^{298}$ for the reaction $Li^+ + H_2O \rightarrow Li(H_2O)^+$ is −34.0 kcal mol^{-1} vs calculated $\Delta H_{\text{hyd}}^{298} = -34.0$ kcal mol^{-1} at the B3LYP/6-311+G(2df,2p)//B3LYP/6-31G* computational level. Similarly, experimental[1] $\Delta H_{\text{hyd}}^{298}$ for $Na^+ = -24.0$ kcal mol^{-1} compared to −23.4 kcal mol^{-1} at the B3LYP/6-311+G(2df,2p)//B3LYP/6-31G* computational level.

Notwithstanding the different computational levels of theory, the trends in the predicted chemical reactivities of the various species are consistent with experimental observations. Our calculations show that the relative affinity of a metal cation for water vs a quinazoline species determines whether a metal−water or metal−quinazoline complex is formed. For example, $\Delta H_{\text{hyd}}^{298}$ for Li^+ is −38.0, −39.3, and −34.0 kcal mol^{-1} at the HF, MP2, and B3LYP level of theory, respectively. The corresponding ΔH_f^{298} for the formation of $Li[C_8H_9N_2O]^{2+}$ complex is 28.8, 27.3, and 32.4 kcal mol^{-1} at the HF, MP2, and B3LYP level of theory, respectively. The data for Na^+ and Ca^{2+} ions (Tables 4 and 5) illustrate the same trends in metal cation reactivity; i.e., hydration is energetically more favorable than metal−quinazoline complex formation. Likewise, the energetics of hydration of metal cations vs hydration of quinazoline species governs the outcome of the competitive hydration reactions. Free energies and enthalpies of hydration at 298.15 K (Table 4) show that metal cation hydration reactions are energetically more favorable than the hydration of quinazoline species. Equally, hydration of protonated quinazoline cations is energetically favored over hydration of neutral quinazoline.

As outlined in Figure 1, hydration of quinazoline involves at least two pathways.[14−19] One pathway involves direct hydration

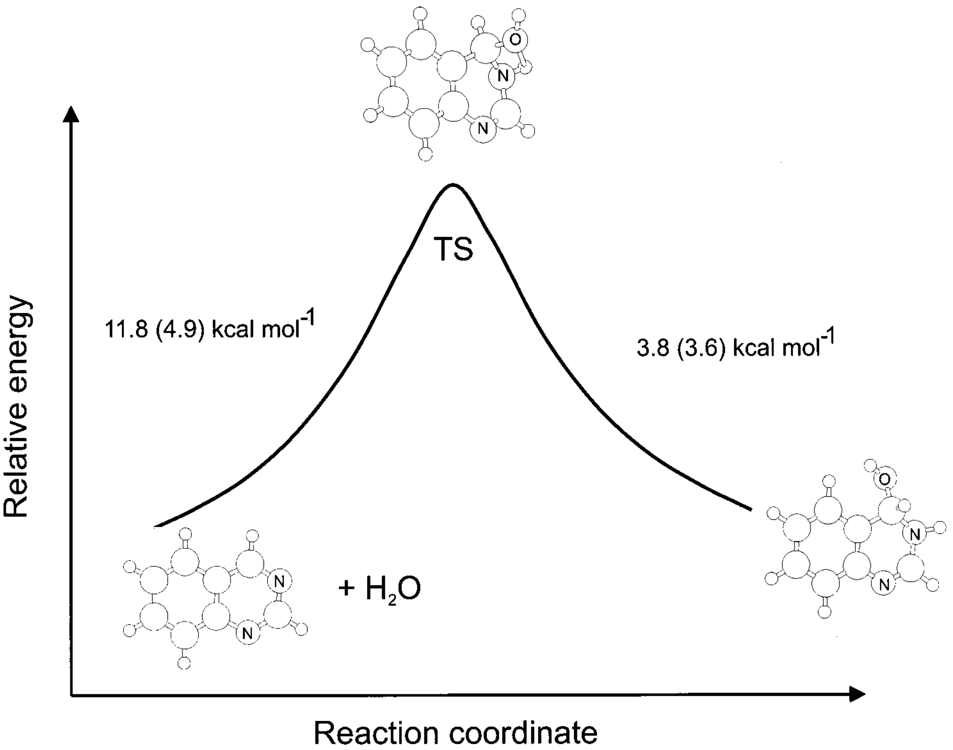

Figure 2. Reaction profile for the hydration of neutral quinazoline showing the calculated activation energies at the B3LYP/6-311+G(2df,2p)//B3LYP/6-31G* level of theory. Activation energies calculated at the MP2/6-31G**//HF/6-31G* level of theory are shown in parentheses. Large unlabeled circles represent carbon atoms, whereas the small circles are hydrogen atoms.

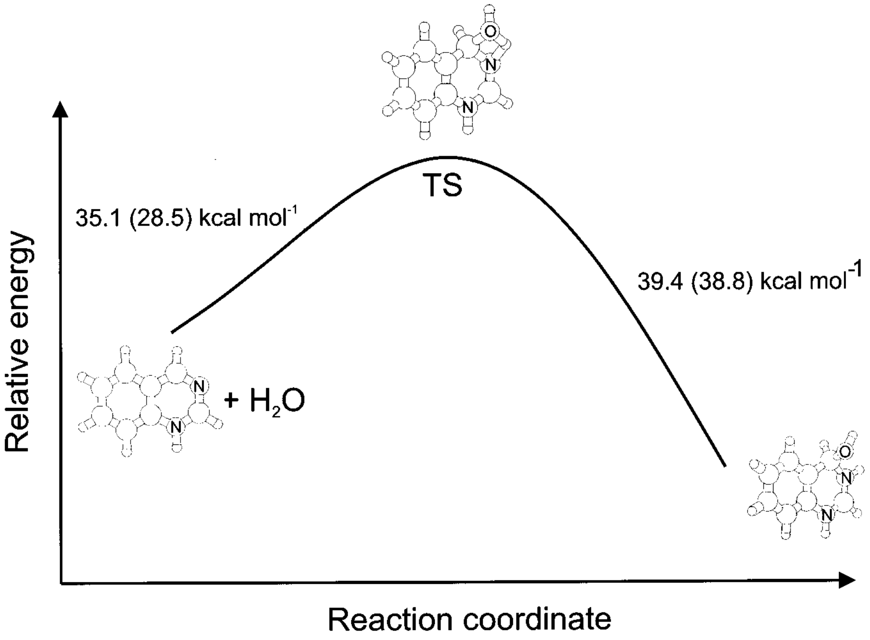

Figure 3. Reaction profile for the hydration of protonated quinazoline (N1) monocation showing the calculated activation energies at the B3LYP/6-311+G(2df,2p)//B3LYP/6-31G* level of theory. Activation energies calculated at the MP2/6-31G**//HF/6-31G* level of theory are shown in parentheses. Large unlabeled circles represent carbon atoms, whereas the small circles are hydrogen atoms.

of quinazoline to 3,4-dihydroquinazolin-4-ol ($K_1 = 5.5 \times 10^{-3}$). The activation energy of the process is 11.8 (4.9) kcal mol^{-1} and 3.8 (3.6) kcal mol^{-1} for the forward and reverse process, respectively, at the B3LYP/6-311+G(2df,2p)//B3LYP/6-31G* (MP2/6-31G**//HF/6-31G*) level of theory. In this pathway, the energetics favors the reverse covalent dehydration process. Moreover, consideration of resonance stabilization energy shows that hydration of neutral quinazoline to form 3,4-dihydroquinazolin-4-ol involves a net loss of ∼−1.2, −0.1, and −4.6 kcal mol^{-1} as computed at HF, MP2, and B3LYP levels of theory, respectively. The influence of resonance stabilization energy was invoked to explain the large differences in the hydration of purine, pteridine, and derivatives.[24] Differences in aromaticity of anhydrous reactants vs hydrous products were found to affect the relative extents of hydration and stability of the heteroaromatic compounds. Therefore, the instability of 3,4-dihydroquinazolin-4-ol is attributable to two factors: (1) the disparity in the relative free energies of the products and reactants, and (2) the loss in resonance energy. Acidification of a 3,4-dihydroquinazolin-4-ol solution generates the stable hydrate cation, 3,4-dihydro-4-hydroxyquinazolin-1-ium ion. However, given the number of favorable competing processes, formation of the quinazoline hydrate cation via this pathway is insignificant.

Next, we consider the other pathways for hydration of quinazoline under acidic conditions. Three species are produced by the protonation of quinazoline, i.e., N1 monocation, N3 monocation, and the dication. The existence of these species was the subject of several experimental investigations,[14−19] and the experimentally determined pK_a's for the various reactions are given in Figure 1. Experimentally, it was assumed that the N3 monocation is slightly more basic than the N1 monocation—based on the fact that isoquinoline (pK_a = 5.42) is a stronger base than quinoline (pK_a = 4.90).[17,18] Because the difference in pK_a values is not very large, a solution of protonated quinazoline is likely a mixture of N1 and N3 monocations, with the N3 monocation being the predominant species. Further protonation of either N1 or N3 monocation forms the dication (pK_a = −5.5). Our stability calculations at the MP2/6-31G**//HF/6-31G* and B3LYP/6-311+G(2df,2p)//B3LYP/6-31G* levels of theory are consistent with the experimental findings, i.e., dication $\gg$ N3 monocation > N1 monocation. However, the difference in energy between N3 and N1 monocations is very small.

Hydration under acidic conditions proceeds by way of water attacking N3, N1, or the dication. Water attack on the N1 monocation proceeds via a pathway involving an intermediate/transition state with a four-atom ring in which hydrogen is partially bonded to both oxygen and nitrogen (see Figure 3). Activation energies for the forward and reverse processes were calculated to be 35.1 (28.5) and 39.4 (38.8) kcal mol^{-1}, respectively, at the B3LYP/6-311+G(2df,2p)//B3LYP/6-31G* (MP2/6-31G**//HF/6-31G*) level of theory. Corresponding experimentally estimated solution phase activation energies at 273 K are 9.3 kcal mol^{-1} for hydration of quinazoline cation and 15.3 kcal mol^{-1} for dehydration of the 3,4-dihydro-4-hydroxyquinazolin-1-ium ion.[17] Unlike hydration of neutral quinazoline, formation of the quinazoline hydrate cation via this pathway is favored.

Conclusion

In a quinazoline−water−metal cation system, the relative affinity for water by the metal cation and quinazoline influences the course of the hydration reactions. Energetic considerations indicate that hydration of Li^+, Na^+, and Ca^{2+} ions is very favorable compared to hydration of quinazoline. What is more, hydration of metal ions prevails over the formation of metal cation−quinazoline complexes. As a result, under very low water content, metal cations out compete quinazoline for water. We also found that hydration of protonated quinazoline is favored over hydration of the neutral species. In fact, 3,4-dihydroquinazolin-4-ol, a product of the covalent hydration of neutral quinazoline is unstable. Loss in resonance energy and the disparity in relative free energies of the products and reactants are considered to be responsible for this instability. Finally, the interaction of the metal cations and quinazoline species with water in the gas phase may provide a basis for more complex interactions in the environment, for example, hydration at clay and metal oxide surfaces. Future work should consider competitive hydration reactions involving, for example, organic contaminant-clay−water systems, heavy metal−clay−water systems, etc. at higher levels of theory.

Acknowledgment. This research was supported, in part, by the National Research Council. This paper has been reviewed in accordance with the U.S. Environmental Protection Agency's peer and administrative review policies and approved for publication. Mention of trade names or commercial products does not constitute endorsement or recommendation for use by the U.S. EPA.

Supporting Information Available: Optimized geometries of all structures. This material is available free of charge via the Internet at http://pubs.acs.org.

References and Notes

(1) Conway, B. E. *Ionic Hydration in Chemistry and Biophysics*; Elsevier: Amsterdam, 1981.
(2) Franks, F. *Water*; Royal Society of Chemistry: London, 1984.
(3) Finney, J. L. *Faraday Discuss*. **1996**, *103*, 1.
(4) Denisov, V. P.; Halle, B. *Faraday Discuss*. **1996**, *103*, 227.
(5) Israelachvili, J.; Wennerström, H. *Nature* **1996**, *379*, 219.
(6) Creighton, T. E. *Proteins: Structures and Molecular Properties*, 2nd ed.; Freeman: New York, 1997.
(7) McBrierty, V. J.; Keely, C. M.; Coyle, F. M.; Xu, H.; Vij, J. K. Denisov, V. P.; Halle, B. *Faraday Discuss*. **1996**, *103*, 255.
(8) Waigh, T. A.; Jenkins, P. J.; Donald, A. M. Denisov, V. P.; Halle, B. *Faraday Discuss*. **1996**, *103*, 325.
(9) Sposito, G.; Prost, R. *Chem. Rev*. **1982**, *82*, 553.
(10) Low, P. F. in *Proceedings of the international Clay Conference, Denver, 1985*; Shultz, L. G., van Olphen, H., Mumpton, F. A., Eds.; The Clays Mineral Society: Bloomington, Indiana, 1987; p 247.
(11) Lasaga, A. C. *Rev. Mineral*. **1990**, *23*, Chapter 2.
(12) Parks, G. A. *Rev. Mineral*. **1990**, *23*, Chapter 4.
(13) Güven, N. *CMS Workshop Lectures* **1992**, *4*, 1.
(14) Albert, A.; Armarego, W. L. F.; Spinner, E. *J. Chem. Soc*. **1961**, 2689.
(15) Albert, A.; Armarego, W. L. F. *Adv. Heterocycl. Chem*. **1965**, *4*, 1.
(16) Perrin, D. D. *Adv. Heterocycl. Chem*. **1965**, *4*, 43.
(17) Bunting, J. W.; Perrin, D. D. *J. Chem. Soc. B* **1967**, 950.
(18) Armarego, W. L. F. In *The Chemistry of Heterocyclic Compounds: Fused Pyrimidines PART 1 Quinazolines*; Brown, D. J., Ed.; Interscience: New York, 1967; Chapter 2.
(19) Albert, A. *Adv. Heterocycl. Chem*. **1976**, *20*, 117.
(20) Bailey, G. W.; Brown, D. S.; Karickhoff, S. W. *Science* **1973**, *182*, 819.
(21) Lepley, A. R.; Chakrabarty, M. R.; Hanrahan, E. S. *J. Chem. Soc. A* **1967**, 1626.
(22) Spedaletti, C. A.; Estrada, M. R.; Yamin, L. J.; Ponce, C. A.; Tomas Vert, F. *An. Asoc. Quim. Argent*. **1990**, *78*, 203.
(23) Erion, M. D.; Reddy, M. R. *J. Comput. Chem*. **1995**, *12*, 1513.
(24) Erion, M. D.; Reddy, M. R. *J. Am. Chem. Soc*. **1998**, *120*, 3295.
(25) Marcus, Y. *J. Chem. Soc., Faraday Trans. 1* **1987**, *83*, 339.
(26) Marcus, Y. *J. Chem. Soc., Faraday Trans*. **1991**, *87*, 2995.
(27) Markham, G. D.; Glusker, J. P.; Bock, C. L.; Trachtman, M.; Bock, C. W. *J. Phys. Chem*. **1996**, *100*, 3488.
(28) Watanabe, H.; Iwata, S. *J. Phys. Chem. A* **1997**, *101*, 487.
(29) Allouche, X. P.; Daudey, J.-P.; Sanejouand, Y.-H. *J. Phys. Chem. B* **1997**, *101*, 5018.
(30) Marcus, Y. *Ion Properties*; Marcel Dekker: New York, 1997.
(31) Pavlov, M.; Siegbahn, P. E. M.; Sandström, M. *J. Phys. Chem. A* **1998**, *102*, 219.
(32) Rodriguez-Cruz, S. E.; Jockusch, R. A.; Williams, E. R. *J. Am. Chem. Soc*. **1998**, *120*, 5842.
(33) Peschke, M.; Blades, A. T.; Kebarle, P. *J. Phys. Chem. A* **1998**, *102*, 9978.
(34) Rodriguez-Cruz, S. E.; Jockusch, R. A.; Williams, E. R. *J. Am. Chem. Soc*. **1999**, *121*, 8898.
(35) Møller, C.; Plesset, M. S. *Phys. Rev*. **1934**, *46*, 618.
(36) Hehre, W. J.; Radom, J.; Pople, A.; Schleyer, P. v. R. *Ab Initio Molecular Orbital Theory*; Wiley: New York, 1986.
(37) Foresman, J. B.; Frisch, A. *Exploring Chemistry with Electronic Structure Methods*, 2nd ed.; Gaussian, Inc.: Pittsburgh, PA. 1996.
(38) Jensen, F. *Introduction to Computational Chemistry*; Wiley: New York, 1999.
(39) Kohn, W.; Sham, L. J. *Phys. Rev*. **1965**, *140*, A1133.
(40) Becke, A. D. *J. Chem. Phys*. **1993**, *98*, 5648.
(41) Lee, C.; Yang, W.; Parr, R. G. *Phys. Rev. B* **1988**, *37*, 785.
(42) Frisch, M. J.; Trucks, G. W.; Schlegel, H. B.; Scuseria, G. E.; Robb, M. A.; Cheeseman, J. R.; Zakrzewski, V. G.; Montgomery, J. A., Jr.; Stratmann, R. E.; Burant, J. C.; Dapprich, S.; Millam, J. M.; Daniels, A. D.; Kudin, K. N.; Strain, M. C.; Farkas, O.; Tomasi, J.; Barone, V.; Cossi, M.; Cammi, R.; Mennucci, B.; Pomelli, C.; Adamo; C.; Clifford, S.;

Ochterski, J.; Petersson, G. A.; Ayala, P. Y.; Cui, Q.; Morokuma, K.; Malick, D. K.; Rabuck, A. D.; Raghavachari, K.; Foresman, J. B.; Cioslowski, J.; Ortiz, J. V.; Baboul, A. G.; Stefanov, B. B.; Liu, G.; Liashenko, A.; Piskorz, P.; Komaromi, I.; Gomperts, R.; Martin, R. L.; Fox, D. J.; Keith, T.; Al-Laham, M. A.; Peng, C. Y.; Nanayakkara, A.; Gonzalez, C.; Challacombe, M.; Gill, P. M. W.; Johnson, B.; Chen, W.; Wong, M. W.; Andres, J. L.; Gonzalez, C.; Head-Gordon, M.; Replogle, E. S.; Pople, J. A. *Gaussian 98*, Revision A.7; Gaussian, Inc.: Pittsburgh, PA, 1998.

(43) Hariharan, P. C.; Pople, J. A. *Chem. Phys. Lett*. **1972**, *16*, 217.

(44) Hariharan, P. C.; Pople, J. A. *Theor. Chim. Acta* **1973**, *28*, 213.

(45) Francl, M. M.; Pietro, W. J.; Hehre, W. J.; Binkley, J. S.; Gordon, M. S.; DeFrees, D. J.; Pople, J. A. *J. Chem. Phys*. **1982**, *77*, 3654.

(46) Peng, C.; Schlegel, H. B. *Isr. J. Chem*. **1993**, *33*, 449.

(47) Peng, C.; Ayala, P. Y.; Schlegel, H. B.; Frisch, M. J. *J. Comput. Chem*. **1996**, *17*, 49.

(48) Gonzalez, C.; Schlegel, H. B. *J. Chem. Phys*. **1989**, *90*, 2154.

(49) Gonzalez, C.; Schlegel, H. B. *J. Phys. Chem*. **1990**, *94*, 5523.

(50) Mclean, A. D.; Chandler, G. S. *J. Chem. Phys*. **1980**, *72*, 5639.

(51) Krishnan, R.; Binkley, J. S.; Seeger, R.; Pople, J. A. *J. Chem. Phys*. **1980**, *72*, 650.

(52) Clark, I.; Chandrasekhar, J.; Spitznagel, G. W.; Schleyer, P. v. R. *J. Comput. Chem*. **1983**, *4*, 294.

(53) Frisch, M. J.; Pople, J. A.; Binkley, J. S. *J. Chem. Phys*. **1984**, *80*, 3265.